Evaluation of movement facilitating techniques for finite element analysis of magnetically geared electrical machines (repository copy)

Article:

Gerber, S., Wang, R-J., (2015) Evaluation of movement facilitating techniques for finite element analysis of magnetically geared electrical machines, *IEEE Transactions on Magnetics*, 51(2): 7400206, February 2015; ISSN: 1941-0069

http://dx.doi.org/10.1109/TMAG.2014.2351787

Evaluation of Movement Facilitating Techniques for Finite Element Analysis of Magnetically Geared Electrical Machines

Stiaan Gerber and Rong-Jie Wang

Department of Electrical and Electronic Engineering, Stellenbosch University, Stellenbosch 7600, South Africa

The simulation of magnetically geared electrical machines using the finite element method is an especially demanding task when movement has to be considered. Several methods that facilitate movement exist. In this paper, two of these methods, the macro air-gap element (AGE) and the moving band (MB) are applied in a time-stepped static simulation of a magnetically geared machine (MGM). The methods are evaluated in terms of accuracy and computational efficiency, vitally important factors for numerical optimization. The implementation of both methods exploit the multi-core architecture of modern CPUs to solve several steps in parallel, drastically reducing the simulation time. Nevertheless, the computational cost of the AGE is prohibitively high in the simulation of MGMs. The MB is computationally efficient and good accuracy can be achieved using a multilayer approach.

***Index Terms*— Air gaps, air-gap element (AGE), computational electromagnetics, electric machines, electromagnetics, finite element analysis, magnetic gears, moving band (MB), parallel programming, permanent magnet machines.**

I. Introduction

MAGNETICALLY geared machines (MGMs) are a new class of electrical machine that integrate a conventional permanent magnet machine with a concentric magnetic gear. These machines are worth considering because of the exceptionally high-torque density that they offer compared with conventional electrical machines. Compared with mechanically geared systems, MGMs promise to be low-maintenance devices with no frictional wear and a long service life. Potential applications include wind power generation [1] and traction motors [2].

An example of an MGM with an inner stator is shown in Fig. 1. Because of the complex layout of these machines and the high number of design variables, a popular approach to designing MGMs is numerical optimization using finite element analysis. In this regard, the computational cost of an analysis is a crucial factor because many analyses are required for optimization. Analyzing MGMs using the finite element method is very demanding for two reasons: 1) the lack of periodicity often necessitates modeling of the full machine and 2) the machines have multiple air gaps (typically two or three) that increase the problem complexity when movement has to be considered.

In this paper, two methods that facilitate movement in finite element meshes are applied to the simulation of the MGM shown in Fig. 1 and evaluated in terms of accuracy and computational efficiency. The methods considered are the air-gap element (AGE) and the moving band (MB).

II. Movement Facilitating Techniques

The methods to be evaluated are briefly described in this section. Although, in this context, the methods are applied in static time-stepped simulations, they are just as applicable to transient analyses such as presented in [3].

Manuscript received April 14, 2014; revised June 19, 2014; accepted August 17, 2014. Date of publication August 28, 2014; date of current version March 20, 2015. Corresponding author: S. Gerber (e-mail: sgerber@sun.ac.za).

Color versions of one or more of the figures in this paper are available online at http://ieeexplore.ieee.org.

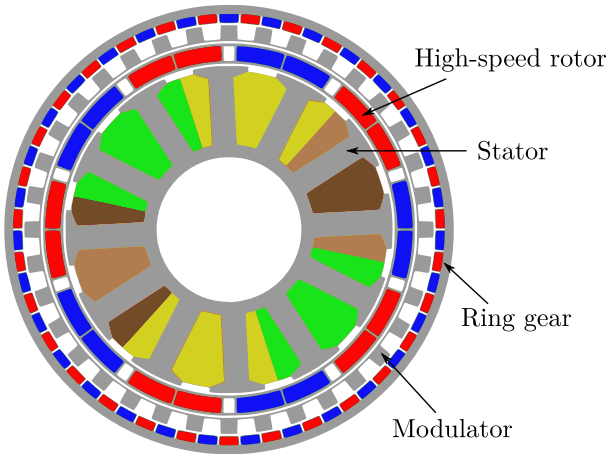

Fig. 1. Example of a magnetically geared permanent magnet machine with an inner stator.

A. Air-Gap Element

The AGE [4] is a technique whereby the field in the entire air-gap region is calculated analytically using a Fourier series expansion of the vector potential. The field representation must satisfy the boundary conditions derived from the adjoining meshed regions. The vector potential in the air gap takes the form

$$A(x,y) = \sum_i \alpha_i(x,y) u_i \tag{1}$$

where the α_i, expressed as Fourier series, fulfill the role of shape functions and the u_i are the nodal values of the vector potential on the AGE boundary. Movement is accomplished by a simple recalculation of the α_i without any modification to the mesh structure, resulting in simple and efficient time-stepping [5].

Considering (1), it is clear that all the air-gap nodes are connected and thus, this method results in a dense block

appearing in the final system matrix that can have a drastic impact on the computational time required to obtain a solution. An advantage of the AGE technique is that the results can be very accurate because of the high order of the field representation in the air-gap region.

The Fourier series representation of the vector potential can be used directly to calculate the torque using the Maxwell stress tensor method

$$T = \frac{L}{\mu_0} \int_{\theta_1}^{\theta_2} r^2 B_r B_\theta d\theta \tag{2}$$

with L the machine's stack length. As described in [6], this calculation can be implemented as

$$T = \frac{L}{\mu_0} \mathbf{A_e}^T \mathbf{F} \mathbf{A_e} \tag{3}$$

with $\mathbf{A_e}$ a vector of nodal values of the vector potential along the boundary of the AGE and $\mathbf{F}$ derived from the Fourier coefficients of the α_i in (1)

$$F_{ij} = r \int_{\theta_1}^{\theta_2} \frac{\partial \alpha_i}{\partial r} \frac{\partial \alpha_j}{\partial \theta} d\theta. \tag{4}$$

Recently, this method has been applied in optimization, where it was used to accurately calculate the gradient of the torque with respect to geometric model parameters [7].

B. Moving Band

This technique was first proposed in [8]. It has several advantages over other movement facilitating methods. It employs no special elements or coupling techniques, no dense blocks are generated in the system matrix and the system dimension is not increased. For these reasons, the MB technique should be superior in terms of computational speed. However, there are difficulties with this method as well; remeshing the air-gap region is inevitable and thus the numbering as well as the amount of nodes in the mesh does not stay constant. For this reason, the conditioning of the system matrix is not maintained and preconditioning routines must be rerun when the mesh changes. In addition, because the elements in the air gap are geometrically distorted or remeshed to accommodate arbitrary movement, the results obtained using this method often have an oscillating error component. It has been shown that this problem can be drastically reduced using higher order elements in the MB [9].

There are a few options for calculating torque in the MB [10]. The Maxwell stress tensor method can also be applied, but in this paper Coulomb's virtual work method [11] was used for torque calculation in the MB

$$T = \frac{L}{\mu_0} \sum_{e=1}^{N_{mb}} \int_{\Omega_e} \left(- \mathbf{B}^T \mathbf{G}^{-1} \frac{\partial \mathbf{G}}{\partial \theta} + \frac{1}{2} \frac{B^2}{|\mathbf{G}|} \frac{\partial |\mathbf{G}|}{\partial \theta} \right) d\Omega \tag{5}$$

with $\mathbf{B} = [B_x, B_y]$, $B = ||\mathbf{B}||$, $\mathbf{G}$ the Jacobian matrix of the global nodal coordinates with respect to local element coordinates, and $|\mathbf{G}|$ the determinant of $\mathbf{G}$.

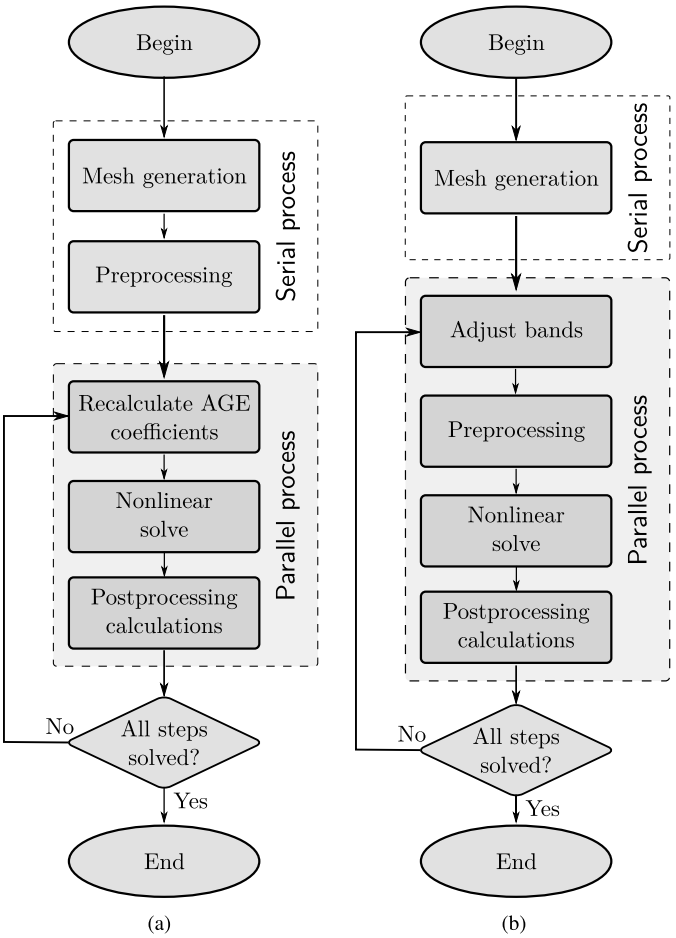

Fig. 2. Flowcharts of different movement facilitating solvers. (a) AGE. (b) MB.

III. Finite Element Implementation

The finite element code used in this paper is an in-house implementation called SEMFEM. The main library is written in Fortran and C and compiled, with optimization, using the GNU compilers *gfortran* and *gcc*.[1] In this section, some details regarding the implementation are discussed.

A. General

First-order triangular elements were used. This is not because any of the methods are restricted to first-order elements, but simply because of the ease of implementation.

A direct method of solving systems of linear equations was used. The implementation is the sub-program ACTCOL listed in [12]. The conditioning of the system is improved before solving using the algorithm proposed in [13]. Newton–Raphson iterations were performed to solve the non-linear system.

B. Solver Implementations

Flowcharts describing the working of the two solvers are shown in Fig. 2. Both solvers comprise a serial section and a parallel section.

The AGE solver utilizes exactly the same mesh for all time-steps, allowing the preprocessing step, which includes

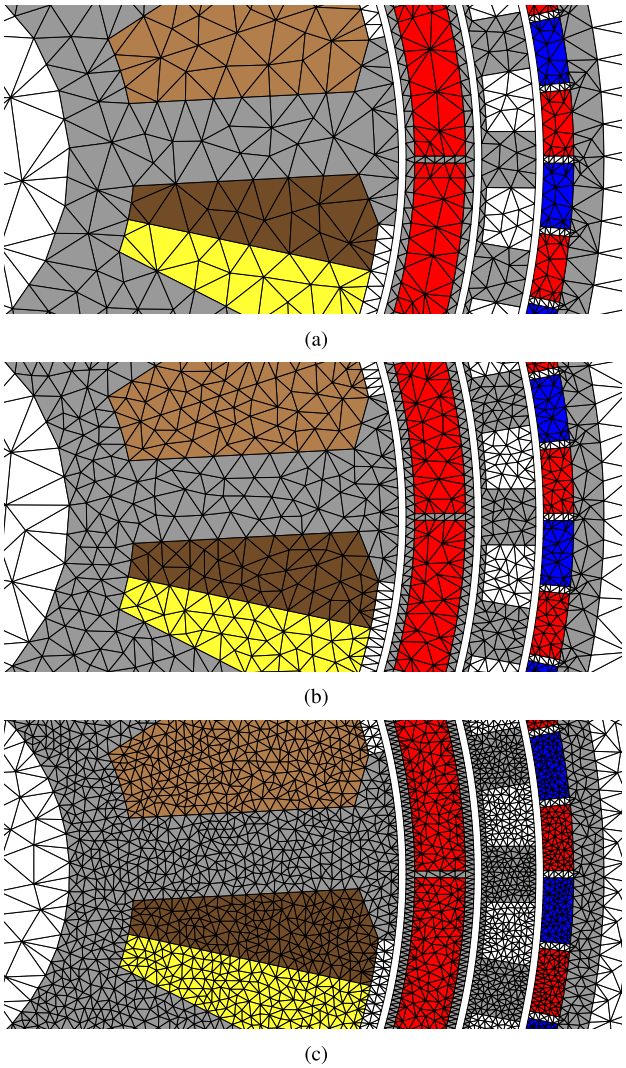

Fig. 3. Three different meshes used for comparison. (a) Mesh 1. (b) Mesh 2. (c) Mesh 3.

profile reduction, to be executed only once. Movement is accomplished by a simple recalculation of some coefficients and updating the entries in the system matrix. On the other hand, the MB solver has to perform the preprocessing step for every time-step, since the connections between nodes in the air-gap region change.

In both methods, the total number of time-steps to be solved are distributed between several parallel sections, implemented using OpenMP [14]. This is a powerful method of parallelization, since it is introduced at a high level. It exploits the fact that time-steps can be solved independently in static time-stepped simulations. As shown in Fig. 2, the non-linear solver and all postprocessing calculations, including the torque calculation, are executed in parallel.

IV. Evaluation

The MGM shown in Fig. 1 was analyzed using both the AGE and the MB. Static time-stepped simulations consisting of 300 time-steps were performed for three different meshes, varying in terms of the density of elements. The meshes are shown in Fig. 3. For Meshes 1 and 2, the MB was setup with

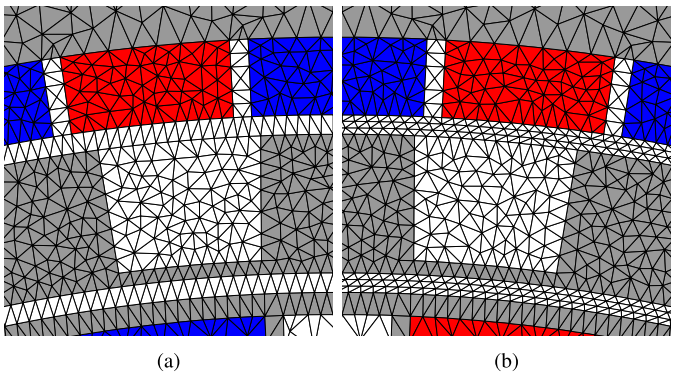

Fig. 4. Variants of the MB technique used with Mesh 3. (a) Single layer: MB1. (b) Triple layer: MB3.

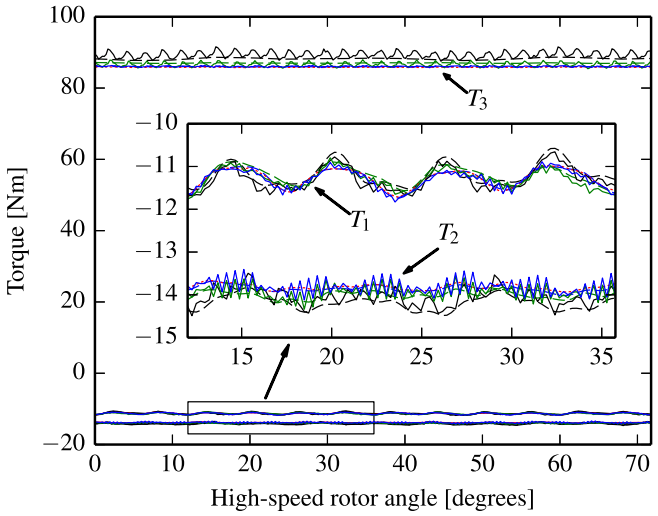

Fig. 5. Comparison of calculated air-gap torques for all simulations.

a single layer of elements (MB1). For Mesh 3, an additional variant of the MB was used with three layers (MB3). Fig. 4 shows the two variants of the MB used with Mesh 3. The MB with three layers was not used for Meshes 1 and 2 because the coarseness of these meshes, together with thin layers in the air gap, results in elements with very poor aspect ratios. Of course, this problem can be avoided by simply refining the air-gap regions, but such refinements are not applied in this paper.

Thus, a total of seven simulations are considered. The simulations were performed at the maximum load angle of the magnetic gear and rated conditions of the stator. Further details regarding the simulated operating point can be found in [15] where the design of the MGM has been described.

The simulations were conducted on a Linux platform using an Intel Core i7 CPU @ 3.5 GHz with four cores (eight virtual cores).

A. Comparison of Accuracy

The torques calculated in the three air gaps for all seven simulations are shown in Fig. 5. The torques in the inner, center, and outer air gaps are labeled T_1, T_2, and T_3, respectively. From this figure, it is apparent that the average torques

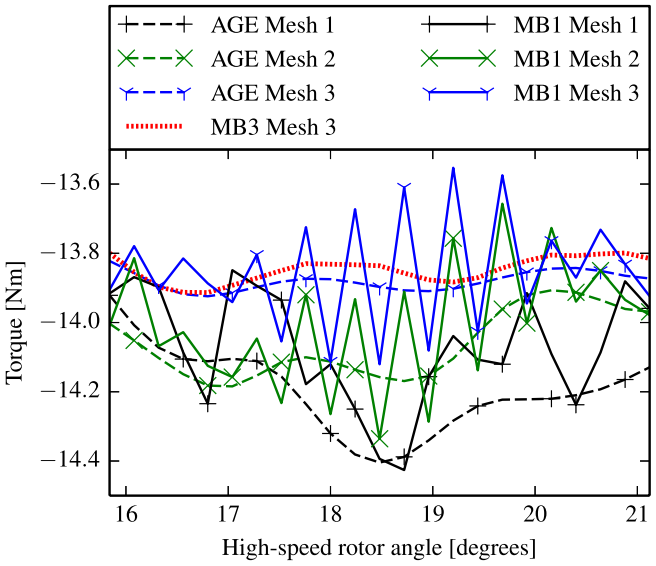

Fig. 6. Close-up view of T_2 calculated using different methods.

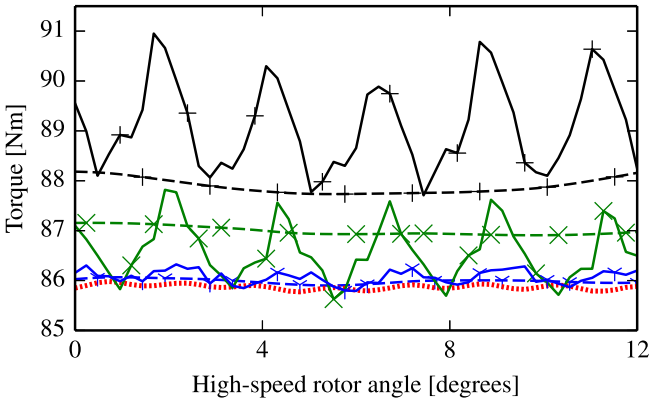

Fig. 7. Close-up view of T_3 calculated using different methods (see Fig. 6 for legend).

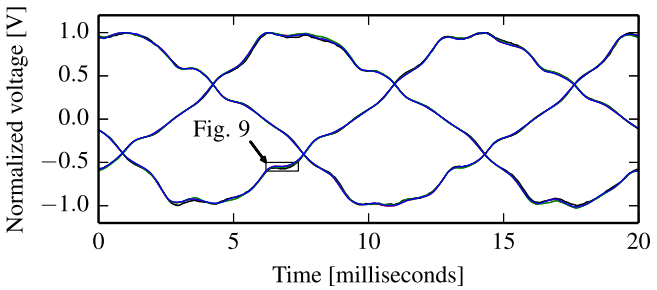

Fig. 8. Comparison of calculated phase voltages for all simulations.

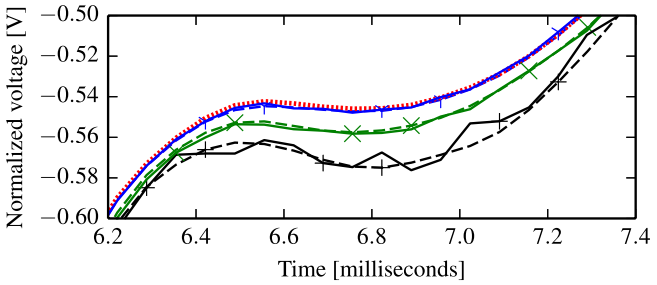

Fig. 9. Close-up view of calculated phase voltages for all simulations (see Fig. 6 for legend).

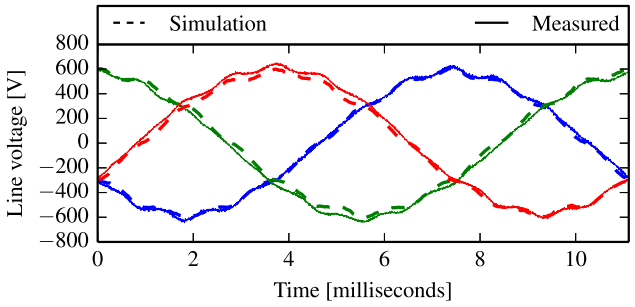

Fig. 10. Comparison of simulated (MB1, Mesh 1) and measured no-load line voltages.

calculated using the different methods and meshes match reasonably well, if not perfectly. However, when one considers the torque ripple, the results from the AGE and the MB differ significantly. In Fig. 5, it can be seen that the largest deviation between the calculated torques occur in T_2 and T_3. Close-up views of T_2 and T_3 are shown in Figs. 6 and 7. The figures share the legend of Fig. 6.

In the case of T_2 (Fig. 6), the MB with a single layer (MB1) produces a high-frequency ripple even with the fine mesh (Mesh 3). This is a good example of the problem mentioned in Section II-B. The deformation and remeshing of the elements result in discontinuities in the problem between the different time-steps. This causes oscillations in the calculated torque. Using the three-layer MB (MB3), these oscillations are dramatically reduced because of the improved smoothness of the solution in the air-gap region. The results show very good agreement between the AGE and MB3 for Mesh 3.

In Fig. 7, the torque ripple calculated using the MB decreases with increasing mesh density. In the case of Mesh 3, the results from the AGE, MB1 and MB3 are in close agreement.

From Figs. 6 and 7, it can be observed that the results from the different methods tend to converge as the mesh density is increased. The variation in average torque is due to the refinement of the mesh in the entire problem domain, not just the air-gap regions.

The three phase voltages calculated for all simulations are shown in Fig. 8. The figure contains seven sets of plots that are indistinguishable from each other in this figure. Fig. 9, which also uses the legend of Fig. 6, shows a close-up view of the voltage waveforms. The figure highlights an area where the difference between the simulations is relatively large. The three groupings of results correspond to the three different meshes. Only in the case of Mesh 1 is there a notable difference between the results from the AGE and the MB. From these results, it can be concluded that the voltage computation is less sensitive to the movement handling scheme than the torque computation. All the methods provide good accuracy in the calculation of flux linkage and voltage.

A comparison of simulated and measured no-load line voltages with the machine's modulator rotating at 150 r/min is shown in Fig. 10. The simulated results were obtained using Mesh 1 with MB1. Despite some inaccuracies in

TABLE I
PERFORMANCE COMPARISON OF MOVEMENT METHODS

Mesh	Calculation times* [seconds]		
	AGE	**MB1**	**MB3**
Mesh 1	1 026.3	99.8	-
(5 722 nodes)	**334.3**	**24.6**	**-**
Mesh 2	3 095.6	305.6	-
(9 860 nodes)	**1 266.8**	**74.7**	**-**
Mesh 3	33 351.5	2 339.4	3 259.2
(28 391 nodes†)	**19 143.5**	**579.6**	**818.9**

* Normal type: 1 thread, bold type: 8 threads
Platform: Linux, Intel Core i7 CPU @ 3.5 GHz, 8 virtual cores
† Excluding additional nodes in the air-gap region using MB 3

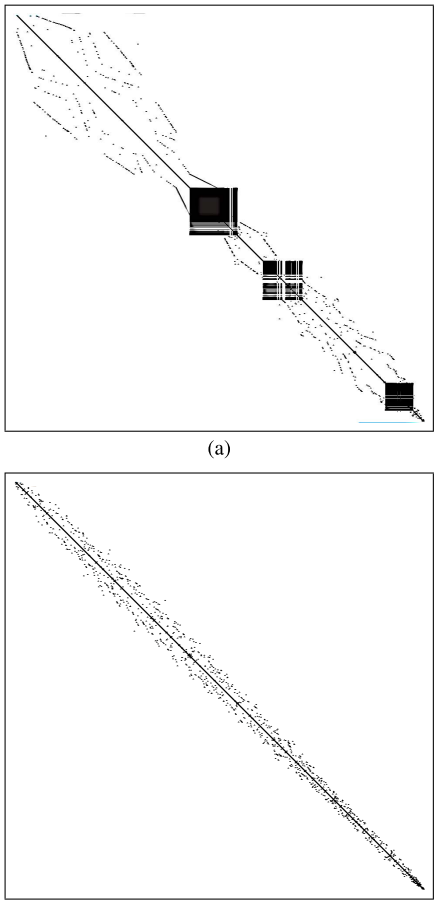

Fig. 11. Matrices generated by FEM. (a) AGE. (b) MB.

the manufacturing of the prototype, these results agree fairly well.

B. Comparison of Performance

The calculation times for the different simulations are given in Table I. The table lists times using a single thread (no parallelism) as well as times for eight threads, which fully exploit the available CPU cores. The calculation times for the MB simulations are consistently reduced by a factor 4 using parallelism. The same speed-up is not quite achieved for the AGE simulations due to the relatively high cost of the preprocessing step, which is not performed in parallel. This effect becomes greater as the mesh density is increased.

Clearly, the MB is much faster than the AGE. Note, also that as the number of nodes in the mesh increases, the margin that the MB has over the AGE increases rapidly. In the simulation of Mesh 1, the MB was roughly 14 times faster, while in the case of Mesh 3, MB1 and MB3 were 33 and 23 times faster, respectively.

The difference in performance between the two methods is far greater than in the simulation of more conventional single air-gap machines. To explain why the MB is so much faster than the AGE when simulating MGMs, Fig. 11 shows the structure of final system matrices obtained using the AGE and the MB. The contribution of the three AGEs are clearly present in the AGE matrix in the form of the three dense blocks. The MB matrix can be solved efficiently using the direct method employed in SEMFEM, but the higher profile and density of the AGE matrix has a great impact on the computational effort required to solve the system. The AGE is especially costly when simulating MGMs because the number of dense blocks are equal to the number of air gaps. Furthermore, the dimensions of the blocks are related to the number of air-gap nodes, which is typically very high in an MGM without periodicity.

V. CONCLUSION

This paper has evaluated two methods of simulating movement in MGMs using the finite element method. Both methods can be executed in parallel, resulting in an appreciable increase in performance. If only the average torque is required as a simulation output, the advantage of using the MB is significant and the accuracy is likely to be sufficient.

The AGE does not suffer from noise associated with distorted elements and for this reason, it may be preferred for torque ripple calculations. The disadvantage of the AGE is its high-computational cost. In the case of MGMs, this cost can be prohibitively high due to the high number of air gaps and lack of periodicity. When accurate torque ripple calculations are required, using the MB with three layers is a good choice.

ACKNOWLEDGMENT

This work was supported in part by ABB Corporate Research, Stockholm, Sweden, in part by the National Research Foundation, South Africa, and in part by Stellenbosch University, Stellenbosch, South Africa.

REFERENCES

[1] C.-T. Liu, H.-Y. Chung, and C.-C. Hwang, "Design assessments of a magnetic-geared double-rotor permanent magnet generator," *IEEE Trans. Magn.*, vol. 50, no. 1, pp. 1–4, Jan. 2014.

[2] K. T. Chau, D. Zhang, J. Z. Jiang, C. Liu, and Y. Zhang, "Design of a magnetic-geared outer-rotor permanent-magnet brushless motor for electric vehicles," *IEEE Trans. Magn.*, vol. 43, no. 6, pp. 2504–2506, Jun. 2007.

[3] S. L. Ho, S. Niu, and W. N. Fu, "Transient analysis of a magnetic gear integrated brushless permanent magnet machine using circuit-field-motion coupled time-stepping finite element method," *IEEE Trans. Magn.*, vol. 46, no. 6, pp. 2074–2077, Jun. 2010.

[4] A. Abdel-Razek, J. I. Coulomb, M. Feliachi, and J. C. Sabonnadiere, "Conception of an air-gap element for the dynamic analysis of the electromagnetic field in electric machines," *IEEE Trans. Magn.*, vol. 18, no. 2, pp. 655–659, Mar. 1982.

[5] T. J. Flack and A. F. Volschenk, "Computational aspects of time-stepping finite-element analysis using an air-gap element," in *Proc. Int. Conf. Elect. Mach.*, Paris, France, 1994, pp. 158–163.

[6] A. A. Abdel-Razek, J. I. Coulomb, M. Feliachi, and J. Sabonnadiere, "The calculation of electromagnetic torque in saturated electric machines within combined numerical and analytical solutions of the field equations," *IEEE Trans. Magn.*, vol. 17, no. 6, pp. 3250–3252, Nov. 1981.

[7] Y. Li and D. C. Aliprantis, "Optimal design of electromechanical devices using a hybrid finite element/air-gap element method," in *Proc. IEEE Power Energy Conf. Illinois (PECI)*, Feb. 2013, pp. 106–113.

[8] B. Davat, Z. Ren, and M. Lajoie-Mazenc, "The movement in field modeling," *IEEE Trans. Magn.*, vol. 21, no. 6, pp. 2296–2298, Nov. 1985.

[9] O. J. Antunes, J. P. A. Bastos, and N. Sadowski, "Using high-order finite elements in problems with movement," *IEEE Trans. Magn.*, vol. 40, no. 2, pp. 529–532, Mar. 2004.

[10] B. Silwal, P. Rasilo, L. Perkkio, A. Hannukainen, T. Eirola, and A. Arkkio, "Evaluation and comparison of different numerical computation methods for the electromagnetic torque in electrical machines," in *Proc. Int. Conf. Elect. Mach. Syst.*, Oct. 2013, pp. 837–842.

[11] J. I. Coulomb and G. Meunier, "Finite element implementation of virtual work principle for magnetic or electric force and torque computation," *IEEE Trans. Magn.*, vol. 20, no. 5, pp. 1894–1896, Sep. 1984.

[12] O. C. Zienkiewicz, *The Finite Element Method*, 3rd ed. England, U.K.: McGraw-Hill, 1977.

[13] N. Gibbs, W. Poole, and P. Stockmeyer, "An algorithm for reducing the bandwidth and profile of a sparse matrix," *SIAM J. Numer. Anal.*, vol. 13, no. 2, pp. 236–250, Apr. 1976.

[14] L. Dagum and R. Menon, "Openmp: An industry-standard API for shared-memory programming," *IEEE Comput. Sci. Eng.*, vol. 5, no. 1, pp. 46–55, Jan. 1998.

[15] S. Gerber and R.-J. Wang, "Design of a magnetically geared PM machine," in *Proc. 4th Int. Conf. Power Eng. Energy Elect. Drives*, Istanbul, Turkey, May 2013, pp. 852–857.